EXPERIMENTAL SIMULATION OF HIGH P-T PLANETARY PROCESSES: PHYSICS OF LASER-INDUCED SHOCKS IN SOLID AND POWDERED TARGETS. J. L. Remo[1,2,3], M. I. Petaev[1,2], and S. B. Jacobsen[1]. [1]Department of Earth and Planetary Sciences, Harvard University, Cambridge MA, [2]Harvard-Smithsonian Center for Astrophysics, Cambridge MA, [3]Sandia National Laboratories, Albuquerque NM.

Introduction: Understanding early evolutions and internal structures of terrestrial and rocky extraterrestrial (so-called Super-Earths [1]) planets requires knowledge of physical and chemical properties of metallic alloys and silicates as well as their interactions at very high pressures and temperatures that are currently beyond the limits of most modern experimental techniques. Recently we reported preliminary results of our laboratory shock experiments [2,3] aimed at understanding metal-silicate interaction at very high temperatures and pressures, comparable to those that may have existed in the deep mantle after the putative Moon-forming giant impact [4]. Here we discuss (1) physical processes taking place in our shock experiments and (2) the approach to calculation of shock parameters such as pressures and temperatures and their gradients.

Experimental setup: The experiments on laser shock-induced melting of metal-dunite targets were conducted at the Sandia National Laboratories using NLS (1064 nm) and ZBL (527 nm) lasers with maximum energy outputs of 660 GW/cm^2 and ~15 TW/cm^2, respectively. The experimental setup [2] allowed an automatic detection of the arrival of the shock wave, monitoring its propagation through the target, and precise measurement of the target rear surface displacement. The rear surface push-out time is measured from the shock wave arrival time to the time taken for the signal to reach its minimal value, indicating complete laser beam displacement from the rear surface probe detector. The real-time electro-optical recordings of the shock wave propagation and particle velocities coupled with the known irradiation intensity were used to calculate the shock parameters discussed below.

Pressures and temperatures in the plasma region and ablation zone: Laser-target interactions generate plasma on target surfaces that expand longitudinally and laterally. The plasma surface is separated from the ablation surface by a plasma region with a critical density that limits wavelength propagation in that region. The absorption of laser light typically occurs close to the critical density at wavelengths longer then ~0.5 μm.

The number density of ions in the critical region, N_c, [5] is related to the radiation wavelength, λ, expressed in micrometers:

$N_c = \pi\, m_e\, c^2/(e^2\lambda^2) = 1.11 \times 10^{21}/\lambda^2$ (ions/cm^3) (1),

where m_e and e are the electron mass and charge, respectively, and c is the speed of light.

Then the critical mass density, ρ_c, is:

$\rho_c = A\, m_p\, N_c /(Z+1)$ (2),

where A is the atomic mass, m_p – the proton mass, and Z – the ionization level.

Substituting for N_c from (1) yields:

$\rho_c = (1.85 \times 10^{-3} A)/((Z+1)\, \lambda^2)$ (g/cm^3) (3).

Because the laser beam penetrated the plasma without significant divergence (scatter), the plasma density of the Sandia ZBL 527 nm laser, ρ_p, should not exceed the critical density, ρ_c; therefore $\rho_p \approx \rho_c = 1.33\times10^{-2}$ g/cm^3.

The pressure, P_c, in the plasma region is defined as:

$P_c = 2\, \rho_c\, v_T^{\,2}$ (Pa) (4),

where v_T is the isothermal sound velocity (*km/s*) in the plasma, which is related to the radiation intensity, I, as:

$I = 4\rho_c\, v_T^{\,3}$ (W/m^2) (5).

Substituting for ρ_c from (3) and v_T from (5) yields:

$P_c = 1.034\times10^{-9}(I/\lambda)^{2/3}(A/(Z+1))^{1/3}$ (GPa) (6).

The temperature in the plasma region, T_c, is defined as:

$T_c = 11.4\, (A/(1+Z))^{1/3}(I\lambda^2)^{2/3}$ (KeV) (7),

with 1 eV = 11,606 K.

At the interface between the plasma region and the ablation region the relevant hydrodynamic conservation conditions of mass and momentum are:

$\rho_c\, v_T = \rho_{abl}\, v_{abl}$ (8)

$P_c + \rho_c\, v_T^{\,2} = P_{abl} + \rho_{abl}\, v_{abl}^{\,2}$ (9).

It is generally assumed [5] that the critical density of the plasma is 10-100× lower than the density of the ablation region underneath it. Accepting a conservative value of 100 ($\rho_c = \rho_{abl}/100$), the boundary condition of $dP \neq 0$ yields:

$\Delta P = P_c - P_{ab} = \rho_{abl}\, v_{abl}^{\,2} - \rho_c\, v_T^{\,2} = -0.99\rho_c\, v_T^{\,2} \approx -\rho_c\, v_T^{\,2}$ (10)

$P_{abl} = P_c + \rho_c\, v_T^{\,2} = 1.5\, P_c$ (11).

Then the temperature in the ablation region, T_{abl}, is defined as:

$T_{abl} = T_c\, (P_{abl}/P_c)(\rho_c/\rho_{abl})$ (12).

The three ZBL targets described in the paper were irradiated with the intensities of 2.2 (ZBL-13), 2.8 (ZBL-16), and 5.8 (ZBL-10) TW/cm^2. For these intensities and the laser wavelength of 527 μm the pressures and temperatures at the top of the ablation zone were 228 GPa and 17,823 K for ZBL-13, 276 GPa and 21,121 K for ZBL-16, and 450 GPa and 34,470 K for ZBL-10. The estimated uncertainties of these values are ~10 rel. %, with the uncertainty of the on-target laser intensity being the main contributor. These values are in a very good agreement (Fig. 1) with the similar experiments on laser-induced shock melting of fused silica and quartz reported by [6] who measured temperatures of shocked materials with an optical pyrometer.

Pressure and temperature gradients within the ablation zones: Rapid attenuation of shock waves propagating through the liquid ablation zone and underlying solid target induce large pressure and temperature gradients in the ablation zone and, to a lesser extent, in the solid target. The temperature gradients across the liquid ablation zones (dT/dz) were calculated using the Fourier's law of heat conduction:

$dT/dz = I_{abl}/\kappa$ and $I_{abl} = \sigma T_{abl}^4$ (13),

where σ is the Stefan-Boltzmann constant and κ is the thermal conductivity of a Si-Fe- Mg-O plasma calculated by the Sesame code [7] for the temperature range of ~4,000 – 40,000 K. The temperature gradients in the ZBL-10, ZBL-13, and ZBL-16 ablation zones are 216, 93, and 67 K/μm, respectively.

The assessment of pressure gradients and, more importantly, the depths of the ablation zones in these samples are more difficult; it appears that only lower and upper limits can be estimated under certain assumptions. The high shock pressures at the top surfaces of the ablations zones drop to rather low Hugoniot pressures of 0.8 and 0.6 GPa measured at the back surfaces of ZBL-13 and ZBL-16, respectively, at room temperature. No Hugoniot pressure for ZBL-10 is available because the target was shattered. Although the travel distances of the shock wave equal to the thicknesses of the targets are known, the thicknesses of the two layers with very different mechanical properties – molten ablation zone and solid porous target – are not. In principle, the ablation zone depths can be evaluated from the known temperature gradients assuming no pressure gradients across the ablation zone. At given pressure the intersection of the temperature profile with either the forsterite or Fe metal melting curve (Fig. 1), whichever is lower, gives the depth of the ablation zone because the shock wave traveling through the deeper portions of a target does not deposit enough energy for melting the target materials. The ablation zone depths estimated this way are 127, 137, and 233 μm for ZBL-10, ZBL-13, and ZBL-16, respectively. The petrographic observations of the recovered ZBL-13 and ZBL-16 targets clearly show that neither olivine nor metal at the crater bottoms experienced pressures and temperatures high enough to produce shock features ubiquitous in shocked meteorites [8]. In particular, the lack of the shock features in the grains of Fe metal points to the peak shock pressures substantially less than a few GPa, implying that the dissipation of the shock energy has occurred over the distances equal to the crater depths or, most likely, even shorter. Assuming that the Hugoniout pressures at the crater bottoms were as low as those recorded at the rear surfaces of the targets, the apparent linear pressure gradients of 0.9465 (ZBL-13) and 0.586 (ZBL-16) GPa/μm were calculated for the crater depths of 240 and 470 μm, respectively. Then the intersections of the pressure-temperature depth profiles with the forsterite melting curve (Fig. 1) give the ablation zone thicknesses of 150 and 250 μm for ZBL-13 and ZBL-16, respectively. These values are only ~ 10 % higher than the depths of the ablation zones calculated under the assumption of no pressure gradients in across the ablation zones.

The estimated depths of the ablation zones in the survived ZBL-13 and ZBL-16 targets imply that the observed craters resulted from two different processes – the initial melting and ablation of the target materials by the laser-induced shock wave followed by the mechanical excavation of shattered target minerals, mainly olivine, after the pressure release.

References: [1] Valencia D. et al. (2006) *Icarus 181*, 545-554. [2] Remo J. L. et al. (2007) *LPS 38*, #1847. [3] Petaev M.I. et al. (2007) *LPS 38*, #1822. [4] Canup R. (2004) *Icarus, 168*, 433-456. [5] Atzeni S. and Meyer-ter-Vehn J. (2004) *The physics of inertial fusion. Beam plasma interaction, hydrodynamics, hot dense matter.* Oxford University Press. [6] Hicks D.G. et al. (2006) *PRL, 97,* 25502-1 to 25502-4. [7] Ramis R. et al (1988) *Comp. Phys. Comm. 49*, 475-481. [8] Stöffler D. et al. (1988) In: *Meteorites and the Early Solar System*, Eds. Kerridge J. F. and Mattews M. S., Univ. Arizona Press, Tucson, 165-202. [9] Luo S.-N. and Ahrens T. J. (2004) *Phys. Earth Planet. Int. 143/144*, 369-386.

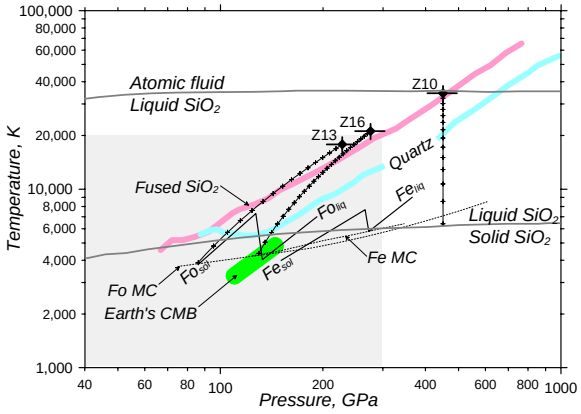

Fig 1: Experimental pressures and temperatures for the ZBL targets are shown by labeled circles with 10% error bars. Black solid lines show the Hugoniots for the solid and liquid forsterite, Fo, and Fe metal, Fe [9]. The dotted lines show the melting curves of Fe metal and forsterite [9]. The Hugoniots for the fused silica and quartz as well as the estimated phase boundaries for solid, liquid and atomic silica fluid are from [6]. The shaded box outlines the P-T space of the Earth-forming giant impact [4]. The solid lines with crosses show T-P profiles across the ablation zones, with the crosses showing depth increase from the top of the ablation zone down to the olivine melting curve with the 10 μm increments.